

MOBILITY AND ACCURACY ANALYSIS OF A CLASS OF OVERCONSTRAINED PARALLEL MECHANISMS

*Nikolay BRATOVANOV**

*Zlatko SOTIROV***

*Vladimir ZAMANOV**

nbratovanov@tu-sofia.bg

ZlatkoS@GenmarkAutomation.com

vzamanov@tu-sofia.bg

*Department "Electrical Motion Automation Systems", TU-Sofia, 1756, BULGARIA**
*Genmark Automation, Inc., CA 94538, USA***

The paper contributes to the mechanics of a class of overconstrained parallel manipulators. It presents an analytical approach to studying the mobility and accuracy of a special type of parallel manipulator, which has found broad industrial application in semiconductor automation. This is a three-degree-of-freedom closed loop mechanism, which exhibits local mobility in close vicinity of specific (singular) configurations. A distinctive feature of this mechanism when in a specific singular configuration is its ability to "use" the inherent elasticity and backlash of its components in order to perform finite small rotations, instead of using additional kinematic joints. The paper provides a formal description of the motion of the mechanism and its accuracy characteristics by analyzing the equations of constraints imposed on its links. The theoretical results are validated by computer simulations and 3D modeling with SolidWorks.

Keywords: *overconstrained closed-loop mechanisms, parallel manipulators, mobility and accuracy analysis, motion simulations, SolidWorks 3D modeling.*

1. Introduction

Parallel manipulators (PM) have gained significant research interest over the last 30 years [Selvi 2012], [Gogu 2008], [Gue et al. 2012], [Sotirov 2002]. Regardless of the fact that many PM have found industrial application, the implementation of overconstrained PM (OCPM) is still limited. In 1996, Genmark Automation, Inc. developed and started to manufacture a special type of OCPM for semiconductor automation. The mechanism was named GPR™ (from "Gimbal Positioning Robot") and was trademarked and patented in 1996 [Genov et al. 1996]. The GPR mechanism had 3 DOF and was designed to perform two small independent rotations in the range of ± 2 degrees and a larger-range (up to 20") translation. The terminal link (platform) was used as a basis for installing serial planar-arms (one or two) with up to 3 DOF each. The resulting hybrid parallel-serial mechanism was capable of adapting to misaligned equipment and compensating for the deflection of the manipulated object, particularly in the case of a very thin object [Genov et al. 1998]. Since 1996, thousands of GPRs have been implemented in various semiconductor FABs, turning out to be one of the largest industrial

implementations of OCPM in the world. A distinctive feature of the overconstrained GPR mechanism is its performance at singular configurations – the ability to "use" the inherent elasticity and backlash of its components in order to perform the required small rotations instead of using additional kinematic joints. In the case of OCPMs, "overconstrained" does not indicate that mechanism does not move; rather, in this case, "overconstrained" indicates that the mechanism has less mobility as required by the manipulating task (i.e. it has motion deficiency in some directions). In other words, specific moves would not exist if the mechanism was ideal, becoming possible only because of its imperfections (inherent elasticities and backlashes of components). Previous paper of the same authors [Bratovanov et al. 2017] proposes how to eliminate this deficiency and provide a formal description of the motion of the mechanism. This paper is an extension of the previous work focusing on more in-depth analysis on the mobility and accuracy of the mechanism.

2. Structure of the GPR™ Mechanism

The GPR mechanism consists of a base and a platform connected by three rods and kinematic

joints. The three rods are parallel and are connected to the base via fifth-order sliding joints. The axes of these joints are parallel. The three rods are connected to the platform via spherical joints. The sliding joints are active and the spherical are passive. There are two orthonormal coordinate frames, $O_b \mathbf{e}_{b1} \mathbf{e}_{b2} \mathbf{e}_{b3}$ and $O_p \mathbf{e}_{p1} \mathbf{e}_{p2} \mathbf{e}_{p3}$, firmly attached to the base and the platform respectively. The centers of the spherical joints are denoted by $P_k, k = 1, 2, 3$ and the intersection points of the sliding joints with the plane of the base passing through the origin O_b are denoted by $B_k, k = 1, 2, 3$. There are also a number of radius-vectors defined:

$\mathbf{r}_{O_b P_k} = (x_{O_b P_k} \ y_{O_b P_k} \ z_{O_b P_k})^T$; $\mathbf{r}_{bk} = \overrightarrow{O_b B_k}$;
 $\mathbf{r}_{pk} = \overrightarrow{O_p P_k}$; $\mathbf{r}_{P_k P_l} = \overrightarrow{P_k P_l}$, see *Figure 1* and *Figure 2*. The length of $\overrightarrow{B_k P_k}$ is denoted by q_k and $\mathbf{q} = (q_1 \ q_2 \ q_3)^T$ is the vector of the generalized coordinates.

3. Mobility Analysis

The position and the orientation of all the links of the mechanism are uniquely defined by a set of parameters $\mathbf{P} \in \mathfrak{R}^N$ which are not necessarily independent. A convenient choice for \mathbf{P} is $(\mathbf{q}^T \ \mathbf{r}_{O_b P_1}^T \ \mathbf{r}_{O_b P_2}^T \ \mathbf{r}_{O_b P_3}^T)^T$. The equations of constraints imposed on \mathbf{P} by the mechanism are:

$$(1) \quad \Phi: \mathfrak{R}^N \rightarrow \mathfrak{R}^N: \Phi(\mathbf{P}) = 0$$

Given the definition of \mathbf{P} , eq. (1) can be rewritten as

$$\begin{aligned} \mathbf{r}_{b1} + q_1 \mathbf{e}_{b3} - \mathbf{r}_{O_b P_1} &= 0 \\ \mathbf{r}_{b2} + q_2 \mathbf{e}_{b3} - \mathbf{r}_{O_b P_2} &= 0 \\ \mathbf{r}_{b3} + q_3 \mathbf{e}_{b3} - \mathbf{r}_{O_b P_3} &= 0 \\ (\mathbf{r}_{O_b P_2} - \mathbf{r}_{O_b P_1})^2 - L_{12}^2 &= 0 \\ (\mathbf{r}_{O_b P_3} - \mathbf{r}_{O_b P_2})^2 - L_{23}^2 &= 0 \\ (\mathbf{r}_{O_b P_1} - \mathbf{r}_{O_b P_3})^2 - L_{31}^2 &= 0 \end{aligned}$$

The Jacobian matrix of $\Phi(\mathbf{P})$ is

$$\frac{d\Phi}{d\mathbf{P}} = \begin{pmatrix} \mathbf{A}_{11} & -\mathbf{I}_3 & \mathbf{0}_3 & \mathbf{0}_3 \\ \mathbf{A}_{21} & \mathbf{0}_3 & -\mathbf{I}_3 & \mathbf{0}_3 \\ \mathbf{A}_{31} & \mathbf{0}_3 & \mathbf{0}_3 & -\mathbf{I}_3 \\ \mathbf{0}_3 & \mathbf{A}_{42} & \mathbf{A}_{43} & \mathbf{A}_{44} \end{pmatrix}$$

$$\mathbf{A}_{11} = \begin{pmatrix} 0 & 0 & 0 \\ 0 & 0 & 0 \\ 1 & 0 & 0 \end{pmatrix}, \mathbf{A}_{21} = \begin{pmatrix} 0 & 0 & 0 \\ 0 & 0 & 0 \\ 0 & 1 & 0 \end{pmatrix}, \mathbf{A}_{31} = \begin{pmatrix} 0 & 0 & 0 \\ 0 & 0 & 0 \\ 0 & 0 & 1 \end{pmatrix}$$

$$\mathbf{A}_{42} = \begin{pmatrix} -2(x_{O_b P_2} - x_{O_b P_1}) & -2(y_{O_b P_2} - y_{O_b P_1}) & -2(z_{O_b P_2} - z_{O_b P_1}) \\ 0 & 0 & 0 \\ 2(x_{O_b P_1} - x_{O_b P_3}) & 2(y_{O_b P_1} - y_{O_b P_3}) & 2(z_{O_b P_1} - z_{O_b P_3}) \end{pmatrix}$$

$$\mathbf{A}_{43} = \begin{pmatrix} 2(x_{O_b P_2} - x_{O_b P_1}) & 2(y_{O_b P_2} - y_{O_b P_1}) & 2(z_{O_b P_2} - z_{O_b P_1}) \\ -2(x_{O_b P_3} - x_{O_b P_2}) & -2(y_{O_b P_3} - y_{O_b P_2}) & -2(z_{O_b P_3} - z_{O_b P_2}) \\ 0 & 0 & 0 \end{pmatrix}$$

$$\mathbf{A}_{44} = \begin{pmatrix} 0 & 0 & 0 \\ 2(x_{O_b P_3} - x_{O_b P_2}) & 2(y_{O_b P_3} - y_{O_b P_2}) & 2(z_{O_b P_3} - z_{O_b P_2}) \\ -2(x_{O_b P_1} - x_{O_b P_3}) & -2(y_{O_b P_1} - y_{O_b P_3}) & -2(z_{O_b P_1} - z_{O_b P_3}) \end{pmatrix}$$

The mobility of the mechanism characterized by its DOF is $h = N - \text{Rank} \left(\frac{d\Phi}{d\mathbf{P}} \right)$ [Jian et al. 2004]. In the case of $q_1 = q_2 = q_3$, $\text{Rank} \left(\frac{d\Phi}{d\mathbf{P}} \right) = 9$ and $h = 3$. In other words, the platform has instantaneous local mobility with dimension 3. Even small differences in the coordinates q_1, q_2, q_3 , which are in the range of the normal deviations from the parallelism of the rods connecting the platform to the base, brings $\text{Rank} \left(\frac{d\Phi}{d\mathbf{P}} \right)$ to 11. This means that the platform has a single DOF at the specific configuration, which is an apparent deficiency. The GPR mechanism is designed to work in a close vicinity of the singular configuration $q_1 = q_2 = q_3$. It has to perform two small (± 1.5 deg) independent rotations of the platform about an axis which lies in the plane of the platform and a vertical translation in a larger-range. Since $\text{Rank} \left(\frac{d\Phi}{d\mathbf{P}} \right)$ is equal to 11 everywhere except for $q_1 = q_2 = q_3$, the constraints imposed to the platform by the spherical joints has to be relieved. In real, this happens naturally because of the imperfection of the joints and the inherent elasticity of the links, which compensates the 2 DOF deficiency. To model this behavior, we introduce three virtual sliding joints at the platform as shown in *Figure 1*. The axes of these joints coincide with the respective radius-vectors $\overrightarrow{O_p P_k}$. The geometry of the GPR mechanism can be represented by the following parameters $\mathbf{X} = (l_1 \ l_2 \ l_3)^T$ and $\mathbf{Y} = (L_{12} \ L_{23} \ L_{31})^T$. At singular configuration $l_1 = l_2 = l_3$ and $L_{12} = L_{23} = L_{31}$, see *Figure 3a*. *Figure 3b* shows a configuration with tilted platform $l_1 \neq l_2 \neq l_3$ and $L_{12} \neq L_{23} \neq L_{31}$. In order to further study the mobility of the GPR mechanism augmented by virtual joints, we introduce a parameter-vector $\Psi = (\mathbf{P}^T \mathbf{Y}^T)^T$, $\Psi \in \mathfrak{R}^{N+3}$ and rewrite the equations of constraints as

$$(2) \quad \Phi(\Psi) = 0$$

It is important to be noted here that contrary to $\text{rank} \left(\frac{d\Phi}{d\mathbf{P}} \right)$, $\text{rank} \left(\frac{d\Phi}{d\Psi} \right)$ is always 12, i.e. it doesn't depend on the "distance" to singularity. Therefore the augmented GPR mechanism has always 3 DOF = $\dim(\Psi) - \text{rank} \left(\frac{d\Phi}{d\Psi} \right)$. Let us differentiate eq. (2) w.r.t. \mathbf{P} and \mathbf{Y} and evaluate the properties of the matrices $\left(\frac{\partial \Phi}{\partial \mathbf{Y}} \right)$ and $\left(\frac{\partial \Phi}{\partial \mathbf{P}} \right)$. The matrix $\left(\frac{\partial \Phi}{\partial \mathbf{Y}} \right)$ can be represented in the form

$$\frac{\partial \Phi}{\partial \mathbf{Y}} = \begin{pmatrix} -2L_{12} & 0 & 0 \\ \mathbf{0}_3 & \mathbf{0}_3 & \mathbf{0}_3 \\ 0 & 0 & -2L_{31} \end{pmatrix}$$

and is always of full rank equal to 3. After rewriting eq. (2) in the form

$$(3) \quad \Phi(\mathbf{P}, \mathbf{Y}) = 0$$

and differentiating we obtain

$$(4) \quad \left(\frac{\partial \Phi}{\partial \mathbf{P}}\right) d\mathbf{P} + \left(\frac{\partial \Phi}{\partial \mathbf{Y}}\right) d\mathbf{Y} = 0$$

Let us consider the singular value decomposition (SVD) [Hogben et al. 2007] of the matrices $\frac{\partial \Phi}{\partial \mathbf{P}} = \mathbf{U}_p \mathbf{S}_p \mathbf{V}_p^T$ and $\frac{\partial \Phi}{\partial \mathbf{Y}} = \mathbf{U}_y \mathbf{S}_y \mathbf{V}_y^T$. The matrices \mathbf{S}_p and \mathbf{S}_y are diagonal containing the singular values of the matrices $\frac{\partial \Phi}{\partial \mathbf{P}}$ and $\frac{\partial \Phi}{\partial \mathbf{Y}}$ respectively: $\mathbf{S}_p = \text{diag}(\sigma_{p1}, \sigma_{p2}, \dots, \sigma_{p11}, 0)$ and $\mathbf{S}_y = \text{diag}(\sigma_{y1}, \sigma_{y2}, \sigma_{y3})$. The singular values are arranged in descending order, i.e. $\sigma_{p1} > \sigma_{p2} > \dots > \sigma_{p11} > 0$ and $\sigma_{y1} > \sigma_{y2} > \sigma_{y3}$. The twelfth singular value of $\frac{\partial \Phi}{\partial \mathbf{P}}$ is always zero since the maximum rank of $\frac{\partial \Phi}{\partial \mathbf{P}}$ is 11. As shown above $\text{rank}\left(\frac{\partial \Phi}{\partial \mathbf{P}}\right)$ is equal to 11 in ‘‘regular’’ configurations, where $q_1 \neq q_2 \neq q_3$, and to 9 at singular configuration ($q_1 = q_2 = q_3$). The smallest non-zero singular value σ_{p11} can be viewed as a measure of the ‘‘distance’’ to singularity. We will show below that the SVD of $\frac{\partial \Phi}{\partial \mathbf{P}}$ and $\frac{\partial \Phi}{\partial \mathbf{Y}}$ can be effectively used in evaluating the sensitivity of the vector \mathbf{P} to variations of the vector \mathbf{Y} . All singular values of $\frac{\partial \Phi}{\partial \mathbf{Y}}$ are different from zero and vary slightly as the mechanism moves. In particular, they are non-zero at singularity. The matrix $\frac{\partial \Phi}{\partial \mathbf{Y}}$ has linearly independent columns and is of full rank equal to 3. Therefore, its Moore-Penrose pseudoinverse [Moore-Penrose pseudoinverse] is

$$\frac{\partial \Phi}{\partial \mathbf{Y}}^\dagger = \left(\frac{\partial \Phi}{\partial \mathbf{Y}}^T \frac{\partial \Phi}{\partial \mathbf{Y}}\right)^{-1} \frac{\partial \Phi}{\partial \mathbf{Y}}^T$$

which is also the left inverse of $\frac{\partial \Phi}{\partial \mathbf{Y}}$, i.e. $\frac{\partial \Phi}{\partial \mathbf{Y}}^\dagger \frac{\partial \Phi}{\partial \mathbf{Y}} = \mathbf{I}_3$. Therefore eq. (4) can be solved for $d\mathbf{Y}$

$$d\mathbf{Y} = -\frac{\partial \Phi}{\partial \mathbf{Y}}^\dagger \frac{\partial \Phi}{\partial \mathbf{P}} d\mathbf{P} = \frac{\partial \mathbf{Y}}{\partial \mathbf{P}} d\mathbf{P}$$

It is seen from the last equation that $\|d\mathbf{Y}\|$ obeys the inequality

$$\sigma^- \left(\frac{\partial \mathbf{Y}}{\partial \mathbf{P}}\right) \|d\mathbf{P}\| \leq \|d\mathbf{Y}\| = \left\| \frac{\partial \mathbf{Y}}{\partial \mathbf{P}} d\mathbf{P} \right\| \leq \sigma^+ \left(\frac{\partial \mathbf{Y}}{\partial \mathbf{P}}\right) \|d\mathbf{P}\|$$

where $\sigma^- \left(\frac{\partial \mathbf{Y}}{\partial \mathbf{P}}\right)$ and $\sigma^+ \left(\frac{\partial \mathbf{Y}}{\partial \mathbf{P}}\right)$ are the smallest and the largest singular values of $\frac{\partial \mathbf{Y}}{\partial \mathbf{P}}$. It is important to be noted here that eq. (4) cannot be resolved for $d\mathbf{P}$ since the matrix $\frac{\partial \Phi}{\partial \mathbf{P}}$ is not of full rank, i.e. its pseudoinverse is not left inverse. In this case we can write the following inequalities

$$\sigma^- \left(\frac{\partial \Phi}{\partial \mathbf{P}}\right) \|d\mathbf{P}\| \leq \left\| \frac{\partial \Phi}{\partial \mathbf{P}} d\mathbf{P} \right\| = \left\| \frac{\partial \Phi}{\partial \mathbf{Y}} d\mathbf{Y} \right\| \leq \sigma^+ \left(\frac{\partial \Phi}{\partial \mathbf{Y}}\right) \|d\mathbf{Y}\|$$

$$(5) \quad \|d\mathbf{Y}\| \geq \frac{\sigma^- \left(\frac{\partial \Phi}{\partial \mathbf{P}}\right)}{\sigma^+ \left(\frac{\partial \Phi}{\partial \mathbf{Y}}\right)} \|d\mathbf{P}\|$$

$$(6) \quad \|d\mathbf{P}\| \leq \frac{\sigma^+ \left(\frac{\partial \Phi}{\partial \mathbf{Y}}\right)}{\sigma^- \left(\frac{\partial \Phi}{\partial \mathbf{P}}\right)} \|d\mathbf{Y}\|$$

The last two inequalities define the lower bound of $\|d\mathbf{Y}\|$ for a given $\|d\mathbf{P}\|$ and the upper bound for $\|d\mathbf{P}\|$ for a given $\|d\mathbf{Y}\|$. Since the virtual kinematic joints introduced in the previous paper are parameterized by the vector \mathbf{X} all the relationships above can be rewritten w.r.t. \mathbf{X} given the definition of the matrix $\frac{\partial \mathbf{Y}}{\partial \mathbf{X}}$

$$\frac{\partial \mathbf{Y}}{\partial \mathbf{X}} = \begin{pmatrix} -(l_1 + 0.5l_2)/L_{12} & -(l_2 + 0.5l_1)/L_{12} & 0 \\ 0 & -(l_2 + 0.5l_3)/L_{23} & -(l_3 + 0.5l_2)/L_{23} \\ -(l_1 + 0.5l_3)/L_{31} & 0 & -(l_3 + 0.5l_1)/L_{31} \end{pmatrix}$$

namely

$$\frac{\partial \Phi}{\partial \mathbf{P}} d\mathbf{P} + \frac{\partial \Phi}{\partial \mathbf{Y}} \frac{\partial \mathbf{Y}}{\partial \mathbf{X}} d\mathbf{X} = 0$$

$$\|d\mathbf{X}\| \geq \frac{\sigma^- \left(\frac{\partial \Phi}{\partial \mathbf{P}}\right)}{\sigma^+ \left(\frac{\partial \Phi}{\partial \mathbf{X}}\right)} \|d\mathbf{P}\|$$

$$\|d\mathbf{P}\| \leq \frac{\sigma^+ \left(\frac{\partial \Phi}{\partial \mathbf{X}}\right)}{\sigma^- \left(\frac{\partial \Phi}{\partial \mathbf{P}}\right)} \|d\mathbf{X}\|$$

4. Accuracy analysis

In this section we will analyze the accuracy of the augmented GPR mechanism. This analysis requires solutions of the direct and inverse kinematic problems at position level. As it is seen from Figure 3b, the center of the platform is shifted in the amount of $d\mathbf{r}$ as a result of the tilting, which in fact can be considered as inaccuracy if not calculated correctly and compensated. In order to solve the direct and the inverse kinematic problems the equations of constraints imposed on \mathbf{X} and \mathbf{Y} and their derivatives have to be studied. The following expressions characterize the relationship between \mathbf{X} , \mathbf{Y} , $\dot{\mathbf{X}}$ and $\dot{\mathbf{Y}}$:

$$(7) \quad \mathbf{F}(\mathbf{X}, \mathbf{Y}) = \mathbf{0}$$

which is the same as

$$\begin{aligned} l_1^2 + l_2^2 + l_1 l_2 - L_{12}^2 &= 0 \\ l_2^2 + l_3^2 + l_2 l_3 - L_{23}^2 &= 0 \\ l_3^2 + l_1^2 + l_3 l_1 - L_{31}^2 &= 0 \end{aligned}$$

$$\frac{\partial \mathbf{F}}{\partial \mathbf{X}} = \begin{pmatrix} 2l_1 + l_2 & 2l_2 + l_1 & 0 \\ 0 & 2l_2 + l_3 & 2l_3 + l_2 \\ 2l_1 + l_3 & 0 & 2l_3 + l_1 \end{pmatrix}$$

$$(8) \quad \frac{\partial \mathbf{F}}{\partial \mathbf{Y}} = \begin{pmatrix} -2L_{12} & 0 & 0 \\ 0 & -2L_{23} & 0 \\ 0 & 0 & -2L_{31} \end{pmatrix}$$

$$(9) \quad \dot{\mathbf{X}} = -\left(\frac{\partial \mathbf{F}}{\partial \mathbf{X}}\right)^{-1} \frac{\partial \mathbf{F}}{\partial \mathbf{Y}} \dot{\mathbf{Y}} = \frac{\partial \mathbf{X}}{\partial \mathbf{Y}}$$

$$(10) \quad \dot{\mathbf{Y}} = -\left(\frac{\partial \mathbf{F}}{\partial \mathbf{Y}}\right)^{-1} \frac{\partial \mathbf{F}}{\partial \mathbf{X}} \dot{\mathbf{X}} = \frac{\partial \mathbf{Y}}{\partial \mathbf{X}} \dot{\mathbf{X}}$$

Solving eq. (7) for \mathbf{X} is not straightforward, requiring the use of the well-known Newton-Euler iterative approach. The solutions for $\dot{\mathbf{X}}$ and $\dot{\mathbf{Y}}$ are explicit and require conventional matrix-operations, including matrix-inversion, see eq. (9) and eq. (10).

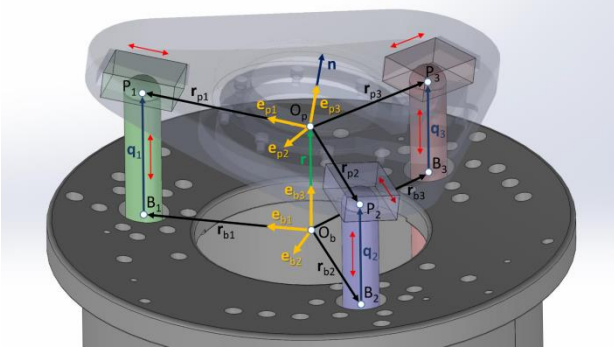


Figure 1. GPR mechanism geometry.

5. Direct Kinematics

Given the generalized coordinates $\mathbf{q} = (q_1 \ q_2 \ q_3)^T$ find the radius-vector \mathbf{r} of the center of the platform O_p with respect to the center of the base O_b and the orientation of the platform represented by its normal vector \mathbf{n} , which coincides with \mathbf{e}_{p3} . The first step of the direct kinematics solution is to solve eq. (7) for \mathbf{X} , given \mathbf{Y}_d . The radius-vectors of the center of the spherical joints at the platform with respect to the center of the base are $\mathbf{r}_{O_b P_1} = \mathbf{r}_{b1} + q_1 \mathbf{e}_{b3}$, $\mathbf{r}_{O_b P_2} = \mathbf{r}_{b2} + q_2 \mathbf{e}_{b3}$ and $\mathbf{r}_{O_b P_3} = \mathbf{r}_{b3} + q_3 \mathbf{e}_{b3}$. The last define the vectors between the centers of the spherical joints at the platform $\mathbf{r}_{P_1 P_2} = \mathbf{r}_{O_b P_2} - \mathbf{r}_{O_b P_1}$, $\mathbf{r}_{P_2 P_3} = \mathbf{r}_{O_b P_3} - \mathbf{r}_{O_b P_2}$ and $\mathbf{r}_{P_3 P_1} = \mathbf{r}_{O_b P_3} - \mathbf{r}_{O_b P_1}$. The components of the desired vector \mathbf{Y} are the Euclidean norms of $\mathbf{r}_{P_1 P_2}$, $\mathbf{r}_{P_2 P_3}$ and $\mathbf{r}_{P_3 P_1}$, which in turn represent the lengths L_{12} , L_{23} and L_{31} respectively:

$$\mathbf{Y}_d = (\|\mathbf{r}_{P_1 P_2}\| \ \|\mathbf{r}_{P_2 P_3}\| \ \|\mathbf{r}_{P_3 P_1}\|)^T$$

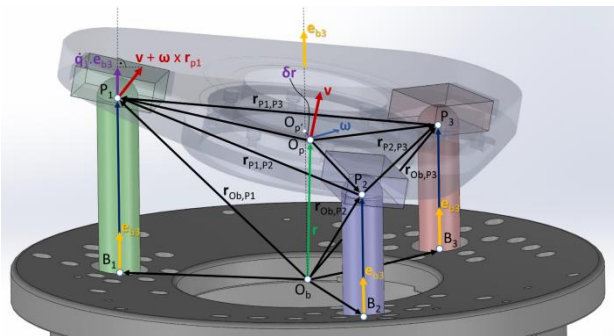


Figure 2. GPR Velocity Distribution.

The initial value of \mathbf{X} corresponds to $q_1 = q_2 = q_3$, i.e. $\mathbf{X}_0 = (R \ R \ R)^T$, where $R = |O_p P_1| = |O_p P_2| = |O_p P_3|$ is the radius of the platform. The

initial value of \mathbf{Y} is $\mathbf{Y}_0 = (R\sqrt{3} \ R\sqrt{3} \ R\sqrt{3})^T$. Given \mathbf{Y}_d , \mathbf{X}_0 and \mathbf{Y}_0 , the value of \mathbf{X} which corresponds to \mathbf{Y}_d is determined via the well-known Newton-Rapson iterative procedure:

$$\mathbf{X}_k = \mathbf{X}_{k-1} + \frac{\partial \mathbf{X}}{\partial \mathbf{Y}} (\mathbf{Y}_d - \mathbf{Y}_{k-1}) \quad k = 1, 2, \dots$$

Normally, it takes 2-3 iterations to find a very accurate solution to the equation $\mathbf{X}_d = \mathbf{X}(\mathbf{Y}_d)$. Once \mathbf{X}_d is found, the calculation of the radius-vector \mathbf{r} of the center of the platform w.r.t. the center of the base and the orientation of the platform becomes straightforward. The unit normal-vector of the platform is calculated as

$$\mathbf{n} = (\mathbf{r}_{P_1 P_2} \times \mathbf{r}_{P_2 P_3}) / \|\mathbf{r}_{P_1 P_2} \times \mathbf{r}_{P_2 P_3}\|$$

and the radius-vector \mathbf{r} as

$$(11) \quad \mathbf{r} = \mathbf{r}_{b1} + q_1 \mathbf{e}_3 + l_1 \cos(\delta) \mathbf{e}_{P_1 P_2} + l_1 \sin(\delta) (\mathbf{n} \times \mathbf{e}_{P_1 P_2})$$

Where

$$\mathbf{e}_{P_1 P_2} = \frac{\mathbf{r}_{P_1 P_2}}{\|\mathbf{r}_{P_1 P_2}\|} \quad \cos(\delta) = \frac{l_1^2 - l_2^2 + L_{12}^2}{2l_1 L_{12}}$$

$$\sin(\delta) = \sqrt{1 - \cos^2(\delta)}$$

6. Inverse Kinematics

Given the position of the platform $\mathbf{z}\mathbf{e}_3$, where $\mathbf{e}_3 = (0 \ 0 \ 1)^T$ and its normal vector \mathbf{n}_d find the length of the rods $\mathbf{q} = (q_1 \ q_2 \ q_3)^T$ connecting the base and the platform. The desired normal vector of the platform \mathbf{n}_d can be obtained by rotating the unit vector \mathbf{e}_3 about $\mathbf{e}_1 = (1 \ 0 \ 0)$ by an angle α and then rotating the resulting vector \mathbf{n}_α about $\mathbf{e}_2 = (0 \ 1 \ 0)$ by an angle β .

$$\mathbf{n}_\alpha = \mathbf{n}_3 \cos(\alpha) + (\mathbf{e}_1 \times \mathbf{n}_3) \sin(\alpha) + \mathbf{e}_1 (\mathbf{e}_1 \cdot \mathbf{n}_3) (1 - \cos(\alpha))$$

$$\mathbf{n}_d = \mathbf{n}_\alpha \cos(\beta) + (\mathbf{e}_2 \times \mathbf{n}_\alpha) \sin(\beta) + \mathbf{e}_2 (\mathbf{e}_2 \cdot \mathbf{n}_\alpha) (1 - \cos(\beta))$$

Then the vector of the generalized coordinates can be determined as

$$(12) \quad \mathbf{q} = \begin{pmatrix} (\mathbf{z}\mathbf{e}_{b3} - \mathbf{r}_{b1}) \cdot \mathbf{n}_d \\ \mathbf{e}_{b3} \cdot \mathbf{n}_d \\ (\mathbf{z}\mathbf{e}_{b3} - \mathbf{r}_{b2}) \cdot \mathbf{n}_d \\ \mathbf{e}_{b3} \cdot \mathbf{n}_d \\ (\mathbf{z}\mathbf{e}_{b3} - \mathbf{r}_{b3}) \cdot \mathbf{n}_d \\ \mathbf{e}_{b3} \cdot \mathbf{n}_d \end{pmatrix}$$

Note that due to the overconstrained nature of the GPR mechanism, the center of the platform may slightly shift with respect to $\mathbf{z}\mathbf{e}_3$. Therefore, once the generalized coordinates according to eq. (12) are found, the actual position of the center of the platform must be calculated through the solution to the direct kinematics problem, see Section 1.

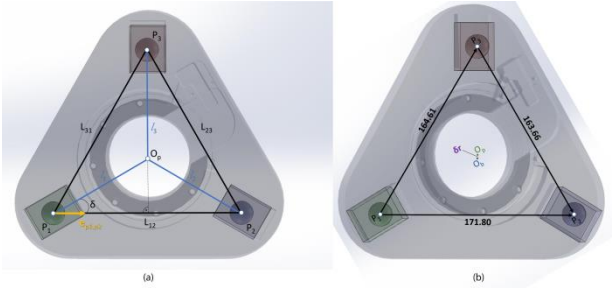


Figure 3. Platform (a) – parallel to the base; (b) – tilted.

7. Simulations

The focus of the simulation study is to evaluate how the singular values of the matrix $\frac{\partial \Phi}{\partial \mathbf{P}}$ and $\frac{\partial \Phi}{\partial \mathbf{Y}}$ change as the mechanism moves and how these singular values are correlated with $d\mathbf{Y}$ and with the range of motion $d\mathbf{X}$ of the virtual joints. In other words – how much of backlash/compliance is needed for the GPR mechanism to guarantee a specific motion $d\mathbf{P}$. In the simulation it was anticipated that $d\mathbf{P} = [0 \ 0 \ 10 \ 0 \ 0 \ 0 \ 0 \ 0 \ 0 \ 0 \ 10]^T$ with norm equal to 14.141 mm.

Specific motion pattern which involves tilting and translation of the platform was selected. It is clearly seen from Figure 4 that during the whole motion the mechanism goes through three singular configurations which allowed studying the performance of the mechanism at these configurations. Figure 5 shows how the smallest singular value $\sigma^- \left(\frac{\partial \Phi}{\partial \mathbf{P}} \right)$ of the matrix $\frac{\partial \Phi}{\partial \mathbf{P}}$ and the norm of the vector $d\mathbf{Y}$ change during the motion of the mechanism. It is clearly seen from this figure that at singular configurations both $\sigma^- \left(\frac{\partial \Phi}{\partial \mathbf{P}} \right)$ and $\|d\mathbf{Y}\|$ take their minimum values of 0.0013 and 0.0181 mm, respectively. The maximum value of $\sigma^- \left(\frac{\partial \Phi}{\partial \mathbf{P}} \right)$ is 0.0871 and of $\|d\mathbf{Y}\|$ is 1.234 mm, which are significantly larger than the respective minimum values. This means that at singularity the “amount” of motion of the virtual joints needed to guarantee motion of the platform in the range specified by $\|d\mathbf{P}\| = 14.14$ mm is 18.1 micron. The singular values $\sigma^- \left(\frac{\partial \Phi}{\partial \mathbf{P}} \right)$, $\sigma^+ \left(\frac{\partial \Phi}{\partial \mathbf{Y}} \right)$ and $\sigma^+ \left(\frac{\partial \Phi}{\partial \mathbf{X}} \right)$ can be used to determine the lower bounds of $\|d\mathbf{Y}\|$ and $\|d\mathbf{X}\|$ corresponding to $\|d\mathbf{P}\| = 14.14$ mm, see Figure 6. The knowledge about these bounds could be very useful during the design and component selection of the mechanism.

Figure 7 is related to the accuracy of the GPR OC mechanism. It shows how the center of the platform moves during rotation of the platform in the range $[-2^\circ, 2^\circ]$. As it is seen from the plot, dx and dy have magnitude of less than 30 micron. The deviation in the vertical direction dz is negligibly small, less than 2 micron (not shown).

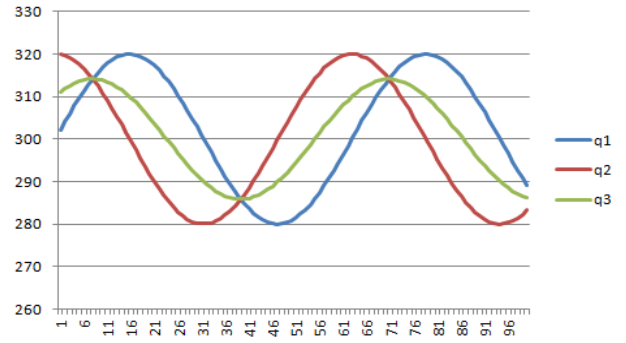


Figure 4. General coordinates used to simulate tilting.

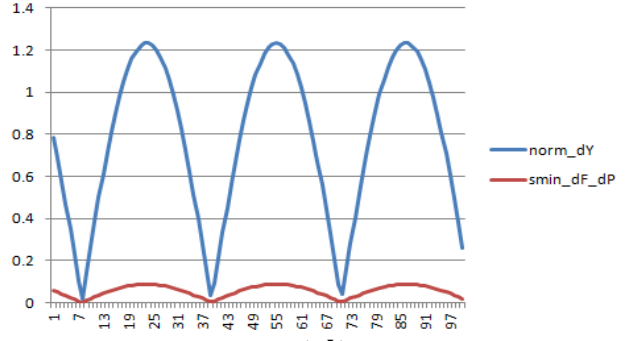


Figure 5. $\|d\mathbf{Y}\|$ and $\sigma^- \left(\frac{\partial \Phi}{\partial \mathbf{P}} \right)$ at each configuration.

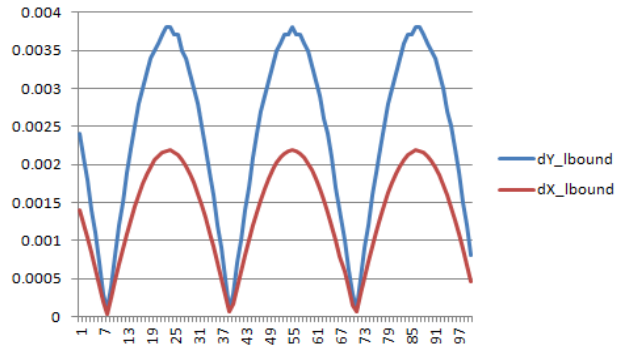


Figure 6. $\|d\mathbf{Y}\|$ and $\|d\mathbf{X}\|$ lower bounds.

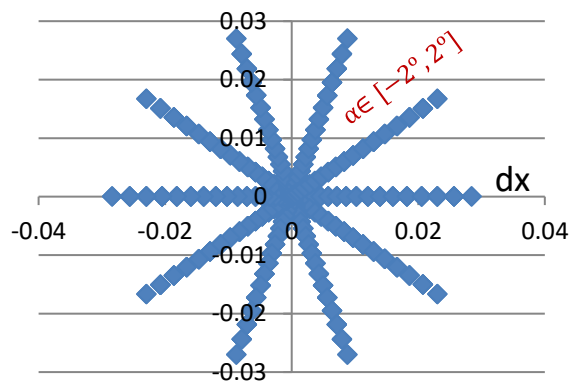


Figure 7. Deviations of the center of the platform.

8. Conclusions

This work further contributes to the mechanics of GPR mechanism and especially to studying its mobility and accuracy in a vicinity of singular configurations. The relationship between the finite rotations of the platform and the imperfections of

the components, connecting the platform and the base was in-depth analyzed by using approaches from the analytical mechanics. The Singular Value Decomposition of the Jacobian matrices of the equations of constraints imposed on the moving platform was found to be an effective tool for determining the relationship between the range of motion of the previously introduced virtual sliding joints and the effective range of motion of the platform. The SVD approach helped at determining the boundaries of the motion of the virtual joints proving to be very small and within the range of the inherent imperfections of the mechanism's components. As in the first paper, the authors acknowledge that there are many different ways for introducing virtual joints and therefore the results obtained in this study are not exhaustive. However the proposed analytical approach to studying the kinematics of the OC GPR mechanism makes a step forward to introducing alternative and higher DOF virtual joints which better represent the effect of backlashes and deformations associated with the mechanism. It is believed that the recent work adds to establishing a basis for future studies in the area of kinematics and dynamics of OCPM.

REFERENCES

Bratovanov, N., Sotirov, Z., Zamanov, V., "Modeling and Simulation of Overconstrained Closed-Loop

Mechanisms", Proceedings of Technical University of Sofia, Vol. 67, No. 2, 2017, p.81-90.

Genov, G., Sotirov, Z., and Bonev, E., "Robot Motion Compensation System", US Patent US6489741B1, August 1998.

Genov, G., Todorov, D., "Universally Tilttable Z-Axis Drive", US Patent US5954840, June 13, 1996.

Grigore GOGU, "Structural and Kinematic Structural and Kinematic Analysis and Synthesis of Analysis and Synthesis of Parallel Robot," SSIR-Clermont-Ferrand - June 27, 2008.

Hogben, L., Rosen, K., "Handbook of Linear Algebra". Taylor & Francis Group, 2007.

Jian S. Dai, Zhen Huang and Harvey Lipkin, "Mobility of Overconstrained Parallel Mechanisms," J. Mech. Des 128(1), 220-229 (Oct 14, 2004).

Moore-Penrose pseudoinverse. In Wikipedia. Retrieved September 06, 2017, from http://en.wikipedia.org/wiki/Moore-Penrose_pseudoinverse

Özgün Selvi, "Structural and kinematic synthesis of overconstrained mechanisms," Ph.D. Thesis, Izmir, 2012.

Sheng Guo, Haibo Qu, Yuefa Fang, Congzhe Wang, "The DOF Degeneration Characteristics of Closed-Loop Overconstrained Mechanisms, Transactions of the Canadian Society for Mechanical Engineering, Vol. 36, No. 1, 2012.

Sotirov, Z.M., "Parallel-Series Manipulators in Semiconductor Automation "Semiconductor European, July 2002.

АНАЛИЗ НА МОБИЛНОСТТА И ТОЧНОСТТА НА КЛАС СВРЪХОГРАНИЧЕНИ ПАРАЛЕЛНИ МЕХАНИЗМИ

Николай БРАТОВАНОВ

Златко СОТИРОВ

Владимир ЗАМАНОВ

Представен е аналитичен подход за изучаване на мобилността и точността на специален тип свръхограничен паралелен манипулатор, намерил широко приложение в автоматизацията на полупроводниковата индустрия. Механизмът е разработен и патентован от фирма Genmark Automation, Inc. през 1996 под наименованието GPR™ (Gimbal Positioning Robot). GPR е затворен механизъм с 3 степени на свобода, състоящ се от основа и платформа (изпълнително звено), свързани помежду си посредством 3 цилиндрични звена (пръти) и 6 кинематични връзки – 3 плъзгащи в основата (активни) и 3 сферични в платформата (пасивни). Платформата може да извършва две малки независими ротации в интервала $\pm 2^\circ$ и една трансляция във вертикално направление с големина до $20''$. Отличителна черта на механизма е способността му да „използва“ еластичността и хлабините на компонентите си за извършването на независимите ротации на платформата (в близка околност на сингулярна конфигурация), елиминирайки нуждата от допълнителни кинематични връзки. Позицията и ориентацията на всички звена на механизма се описват

еднозначно с помощта на вектора \mathbf{P} , съдържащ 12 параметъра $(\mathbf{q}^T \mathbf{r}_{O_b P_1}^T \mathbf{r}_{O_b P_2}^T \mathbf{r}_{O_b P_3}^T)^T$, където \mathbf{q}^T е векторът на обобщените координати q_1, q_2, q_3 , а $\mathbf{r}_{O_b P_1}^T \mathbf{r}_{O_b P_2}^T \mathbf{r}_{O_b P_3}^T$ са векторите, свързващи центъра на основата O_b с центъра на съответните сферични стави P_1, P_2 и P_3 (фиг. 1, фиг. 2). Мобилността на механизма се изследва чрез анализирани на уравненията на геометричните връзки $\Phi(\mathbf{P}) = 0$ и тяхната матрица на Якоби $\frac{d\Phi}{d\mathbf{P}}$. Известно е, че броят на степените на свобода на механизма (h) е равен на разликата на размерността на вектора \mathbf{P} ($N=12$) и ранга на матрицата $\frac{d\Phi}{d\mathbf{P}}$: $h = N - \text{rank} \left(\frac{d\Phi}{d\mathbf{P}} \right)$. В случая, когато $q_1 = q_2 = q_3$, $\text{rank} \left(\frac{d\Phi}{d\mathbf{P}} \right) = 9$ и $h = 3$. С други думи, платформата има локална мобилност с размерност 3. Дори минимални отклонения на q_1, q_2 или q_3 довеждат до $\text{rank} \left(\frac{d\Phi}{d\mathbf{P}} \right) = 11$, което означава, че броят на степените на свобода на механизма за всяка конфигурация, различна от сингулярната ($q_1 = q_2 = q_3$), е равен на 1. На практика този очевиден недостиг на 2 степени на свобода, наложен от геометричните връзки на механизма, се преодолява по естествен начин благодарение на несвършенствата на сферичните лагери и еластичността на компонентите. Моделирането на това поведение се осъществява чрез въвеждане на виртуални плъзгащи връзки към структурно-кинематичния модел на механизма, показани на фиг. 1. С тяхна помощ е възможно количествено да се определи зависимостта между движението на платформата ($\|d\mathbf{P}\|$) и необходимите хлабини и деформации на компонентите ($\|d\mathbf{X}\|, \|d\mathbf{Y}\|$). Изследва се и нежеланото изместване на центъра на платформата O_p спрямо центъра на основата O_b , породено от свръхограничената структура на механизма. За целта се решават правата и обратната задачи на кинематиката на ниво позиция. В допълнение, мобилността на GPR се изследва и чрез метода за декомпозиция по сингулярни стойности на матрицата на Якоби $\frac{\partial \Phi}{\partial \mathbf{P}}$. Тъй като нейният ранг не може да бъде по-голям от 11, дванадесетото сингулярно число σ_{p12} е винаги равно на 0 (при всяка „регулярна“ конфигурация на механизма). С доближаването към „сингулярна“ конфигурация стойностите на двете най-малки ненулеви сингулярни числа σ_{p10} и σ_{p11} намаляват, достигайки 0 именно при $q_1 = q_2 = q_3$. В този смисъл σ_{p10} и σ_{p11} могат да бъдат разглеждани като показател за близостта до „сингулярна“ конфигурация на механизма. Установява се, че метода за декомпозиция по сингулярни стойности е ефективен инструмент за изследването на мобилността на GPR и за анализиранието на връзката между големината и обхвата на движение на виртуалните връзки, изразяващи хлабините и деформациите на компонентите ($\|d\mathbf{X}\|, \|d\mathbf{Y}\|$), и желаното преместване на платформата ($\|d\mathbf{P}\|$). Предложеният подход за моделиране на GPR механизма се верифицира чрез компютърни симулации и SolidWorks модел. Фокусът е изследване на изменението на сингулярните стойности на матриците $\frac{\partial \Phi}{\partial \mathbf{P}}$ и $\frac{\partial \Phi}{\partial \mathbf{Y}}$ при осъществяването на конкретни движения на платформата, и количествено установяване на необходимите хлабини и деформации. За целта се симулира примерно движение, състоящо се в преместване на обобщената координата q_3 на разстояние 10mm като се анализират голям брой различни начални конфигурации, в това число 3 сингулярни (фиг. 4). От резултатите (фиг. 5, фиг. 6) става ясно, че именно в „особените“ конфигурации най-малкото сингулярно число $\sigma^- \left(\frac{\partial \Phi}{\partial \mathbf{P}} \right)$ на матрицата $\frac{\partial \Phi}{\partial \mathbf{P}}$, както и нормата $\|d\mathbf{Y}\|$ имат минимални стойности. Това означава, че в тези конфигурации желаното преместване на платформата $\|d\mathbf{P}\|$ се осъществява с минимални премествания на виртуалните връзки $\|d\mathbf{Y}\|$ – или в реалния случай – с минимални хлабини и деформации на компонентите. Големината на преместването на центъра на платформата O_p спрямо центъра на основата O_b се изследва, чрез решаване на задачите на кинематиката. За целта се симулира втори тип движение, състоящо се в последователно наклоняване на платформата на $\pm 2^\circ$, стартирайки от различни начални конфигурации. Установява се, че отклоненията в равнината (dx, dy) са с големина около 30mm, докато тези във вертикално направление (dz) са пренебрежимо малки (по-малки от 2mm).